Photofragment Translational Spectroscopy of 1-Bromo-3-fluorobenzene and 1-Bromo-4-fluorobenzene at 266 nm

Xi-Bin Gu, Guang-Jun Wang, Jian-Hua Huang, Ke-Li Han,* Guo-Zhong He, and Nan-Quan Lou

State Key Laboratory of Molecular Reaction Dynamics, Dalian Institute of Chemical Physics, Chinese Academy of Sciences, Dalian 116023, China

Received: September 25, 2000

The ultraviolet photodissociation of 1-bromo-3-fluorobenzene and 1-bromo-4-fluorobenzene at 266 nm has been performed on a universal crossed molecular beams machine combined with the photofragment translational spectroscopy (PTS) detection technique. The time-of-flight (TOF) spectra of Br and FC_6H_4 photofragments have been measured. The observed translational energy distributions $P(E_t)$ of photofragments revealed that about 46.8 ± 3.3% and 41.7 ± 3.0% of the available energy are partitioned into translational energy and the anisotropy parameter β is 0.7 ± 0.1 and −0.4 ± 0.1 for 1-bromo-3-fluorobenzene and 1-bromo-4-fluorobenzene, in accord with that of bromobenzene (−0.7), indicating significant change caused by the fluorine atom substitution. To better interpret the experimental results, ab initio calculations have been performed and the calculation results are in good agreement with the experimental results. A plausible photodissociation mechanism is suggested, and the substitution effect of the fluorine atom is discussed.

1. Introduction

Molecular photodissociation has developed into an important field over the past decades.[1,2] The investigation of the photodissociation of polyatomic molecules is an important step toward the understanding of the microscopic dynamics of chemical reactions,[1,3] laser-induced chemistry, photochemical lasers, and atmospheric reaction cycles. The time-of-flight (TOF)[4,5] photofragment translational spectroscopy (PTS)[6−9] method has provided an ideal tool to investigate these photodissociation dynamics in a collision-free regime, in which any neutral photofragment (stable molecule or reactive radical) can be detected. This is particularly suitable for polyatomic photofragments that are difficult to be probed directly by state-specific optical methods such as laser-induced fluorescence (LIF) and resonance-enhanced multiphoton ionization (REMPI), etc. The second important measurable quantity is the angular distribution of the photofragment with respect to the electric vector of the photolysis light. Knowledge of this property allows the symmetry of the excited state as well as the time scale of photodissociation to be inferred.[2,11−16] The third advantage is that, in some cases, the method can deduce the internal energy, such as vibrational[17−21] or rotational[22] energy distributions, with sufficiently high resolution to resolve these internal degrees of freedom by measuring the photofragment recoil speed distributions, based upon energy conservation.

Recently, the photodissociation of a series of aryl halides and alkyl halides[16,23−35] has been performed at different wavelengths by several groups using the PTS technique. The general viewpoint about the dissociation mechanism is that aryl halides undergo predissociation, in contrast to the direct dissociation of alkyl halides. Some alkyl halides such as CH_3Cl,[36,37] CH_3Br,[38] CH_3I[19,39,40] CH_2BrI,[41,42] etc. have been well investigated by PTS, and the results reveal that these molecules undergo fast photodissociation by a transition to the repulsive (n,σ*) state, leading to a direct dissociation with concomitant large translational energy release. However, in the case of aryl halides, the dissociation process is more complicated because multiple channels and more electronic states may be involved. The early experimental results have shown that predissociation seems dominant over direct dissociation, and the dissociation is suggested to be completed on a picosecond time scale.[16,29,43,44] The lifetimes of the dissociating states of the aryl iodides are a little longer than a molecular rotation period, i.e. ∼1 ps; aryl bromides dissociate on a time scale much longer than aryl iodides. Moreover, the photodissociation dynamics of aryl halides depends not only on the halogen atom itself but also on other substituents and the position of them. Therefore, it is very important to study the effects of different substituents and the effects of different positions. In the photodissociation of chlorotoluenes and dichlorobenzenes,[34] the probability of each photodissociation channel is different due to the different substituent and the position of substitution.

For alkyl halides, the substitution effect has been extensively studied, especially for alkyl iodides of small size[39,40,45−51] and their halogenated substituents.[52,53] However, for aryl halides, this kind of substitution effect is seldom studied,[16,34,44,54] particularly for aryl bromides. This paper will discuss the photodissociation dynamics and the substitution effect of fluorine for 1-bromo-3-fluorobenzene and 1-bromo-4-fluorobenzene photodissociation at 266 nm.

2. Experimental Section

The universal crossed molecular beam machine used for the present experiment, which can be used to investigate both reaction scattering and photodissociation dynamics, is one of the most important instruments for studying reaction dynamics; it has been described previously.[55] Moreover, the instrument includes two perpendicular supersonic beams, a main chamber and a rotatable quadrupole mass spectrometer that is operated

* Corresponding author; email: klhan@ms.dicp.ac.cn

10.1021/jp003479q CCC: $20.00
Published on Web 12/22/2000

TABLE 1: Velocity Distributions of Parent Molecules in Supersonic Beam[a]

	α (m/s)	S	v_{pk} (m/s)
1-bromo-3-fluorobenzene	307.1	2.380	842.8
1-bromo-4-fluorobenzene	266.6	2.599	783.6

[a] Velocity distributions are assumed to be $N(v) \propto v^2 * \exp[-(v/\alpha - S)^2]$ and the most probability velocity is $v_{pk} = 0.5 * \alpha * S[1+(1+4/S^2)^{1/2}]$. α and S are adjustable parameters

under high-vacuum conditions. To investigate photofragmentation dynamics, a laser beam replaces one of the supersonic beams.

In brief, the seeded supersonic molecular beam is perpendicularly illuminated by a pulsed laser beam in the main chamber, in which the pressure is kept under 2.0×10^{-4} Pa. The photofragments are ionized by a Brink electron bombardment ionizer and analyzed by a quadrupole mass filter and then detected by a Daly type ion counter consisting of a 30 kV ion target, a scintillator and a photomultiplier. The signals are preamplified and discriminated and then recorded by a 4096 channel multichannel scaler (MCS) with a dwell time of 2 μs, installed in a PC computer. The flight path from the interaction region to the center of the electron impact ionizer is 19.2 cm. The detector can be rotated from −8° to 110° in the plane of the laser and molecular beam with respect to the molecular beam, and is triply pumped by three ion pumps to ensure that the pressure in ionizer region is under 10^{-8} Pa. The continuous supersonic molecular beam is prepared by seeding the reagent in helium and expanding the mixture into the source chamber through a 0.20 mm nozzle. The 266 nm output of a Nd:YAG laser is used and focused to spot size of 2×3 mm^2 at the point of the laser and molecular beam intersection. The laser is operated at a repetition rate of 10 Hz and the laser pulse energy is carefully adjusted and kept at 40 mJ to obtain best signal-to-noise ratio. The TOF spectra are measured at different detector angles corresponding to the molecular beam and the photofragment angular distribution is obtained through integration of the TOF spectra at different angles. The 1-bromo-3-fluorobenzene and 1-bromo-4-fluorobenzene (stated purity ≥ 99%) are obtained from Aldrich Chemical Co. Inc. and used without further purification.

The velocity distributions of parent molecules are measured by chopping the seeded beam with a rotating disk with a slit (1 mm) to get the TOF spectra and fitting them with the program KELVIN.[56] The velocity distribution of supersonic molecular beam is assumed to be $N(v) \propto v^2 * \exp[-(v/\alpha - S)^2]$[57] and the peak (most probable) velocity is given by $v_{pk} = 0.5 * \alpha * S[1 + (1 + 4/S^2)^{1/2}]$.[57] Values of α, *S* and v_{pk} are presented in Table 1.

3. Analysis and Results

3.1. TOF Spectra and Angular Distribution of Photofragment. The photofragment TOF spectra of the two compounds, which are shown in Figure 1 and Figure 2 (open circles), are measured at different angles at $m/e = 80$ corresponding to Br atom and $m/e = 95$ to FC_6H_4. There are two main Br isotopes (^{79}Br and ^{81}Br). In this experiment, we carefully adjust the mass spectrometer to get the best signal-to-noise ratio and find that $m/e = 80$ is very suitable for Br atom. The abscissa indicates the flight time of neutral fragments and the ordinate indicates the signal corresponding to relative intensity.

The solid lines in Figure 1 and Figure 2 represent the calculated TOF spectra through the forward convolution method[58,59] using the program of CMLAB2. The keystone of the forward convolution method is to fit the TOF spectra at different angles and the angular distribution simultaneously by adjusting the total translational energy distribution of the center of mass (CM) and anisotropy parameter. The CM angular distribution is[60]

$$\omega(\theta) = \frac{1}{4\pi}[1 + \beta P_2(\cos\theta)] \quad (1)$$

in which β is the anisotropy parameter whose range is [−1,2], $P_2(\cos\theta)$ is the second-order Legendre polynomial, and θ is the angle between the electric vector of the laser field and the recoiling direction of the photofragment in the CM frame. The parameter β has been analyzed by many groups for various molecules.[6,13,15,60−62] In general, β has the form[15]

$$\beta = yP_2(\cos\chi) \quad (2)$$

where χ is the angle between the transition moment and the recoil axis of the two counterfragments; *y* is a factor related to the lifetime (τ) of the dissociative state. If the molecule dissociates promptly upon absorption of a photon and the recoil kinetic energy is large compared to the energy of rotation, the parameter *y* has the maximum value 2. With increasing lifetime, the parameter *y* decreases monotonically. From the β value, one cannot simultaneously determine the dissociation lifetime τ and the χ value, but one can determine the range of χ. If β is positive, the C−Br bond makes an angle $\chi < 54.7°$ with respect to the transition dipole moment and if β is negative, the C−Br bond makes an angle $\chi > 54.7°$. Two extreme situations are $\beta = 2$ and $\beta = -1$ corresponding to $\chi = 0°$ (parallel transition) and $\chi = 90°$ (perpendicular transition), respectively. In our case, for 1-bromo-3-fluorobenzene, the best-fitted anisotropy parameter β is 0.7 ± 0.1, which indicates that the parallel transition plays an important role in 1-bromo-3-fluorobenzene photodissociation at 266 nm and for 1-bromo-4-fluorobenzene, it is −0.4 ± 0.1, which indicates that the perpendicular transition is dominant over the parallel transition for 1-bromo-4-fluorobenzene photodissociation at 266 nm.

With the best-fitted anisotropy parameter β and the translational energy distribution shown in Figure 4, we obtain the laboratory angular distributions shown in Figure 3 using a least-squares fitting program, which agrees well with the experimental results.

3.2. Translational Energy Distributions. The CM total translational energy distributions of 1-bromo-3-fluorobenzene and 1-bromo-4-fluorobenzene are shown in Figure 4 (A) and (B). The average translational energies $\langle E_t \rangle$ of 1-bromo-3-fluorobenzene and 1-bromo-4-fluorobenzene are 56.76 ± 4.0 kJ/mol and 55.84 ± 4.0 kJ/mol, respectively.

According to the conservation of energy,

$$h\nu + W_{int} - D_0(\text{C}-\text{Br}) = E_t + E_{int} = E_{avl} \quad (3)$$

where $h\nu$ is the photon energy (450.0 kJ/mol), W_{int} is the internal energy of the parent molecule, D_0(C−Br) is the dissociation energy of C−Br bond, E_t denotes the translational energy of photofragment, E_{int} is the internal energy of the fragments, and E_{avl} is the available energy. Thus D_0(C−Br) can be written as

$$D_0(\text{C}-\text{Br}) = h\nu + W_{int} - E_t - E_{int} \quad (4)$$

In our experiment, the internal energy of the parent molecule (W_{int}) can be neglected because a supersonic molecular beam is employed. When E_t becomes a maximum value, the value of

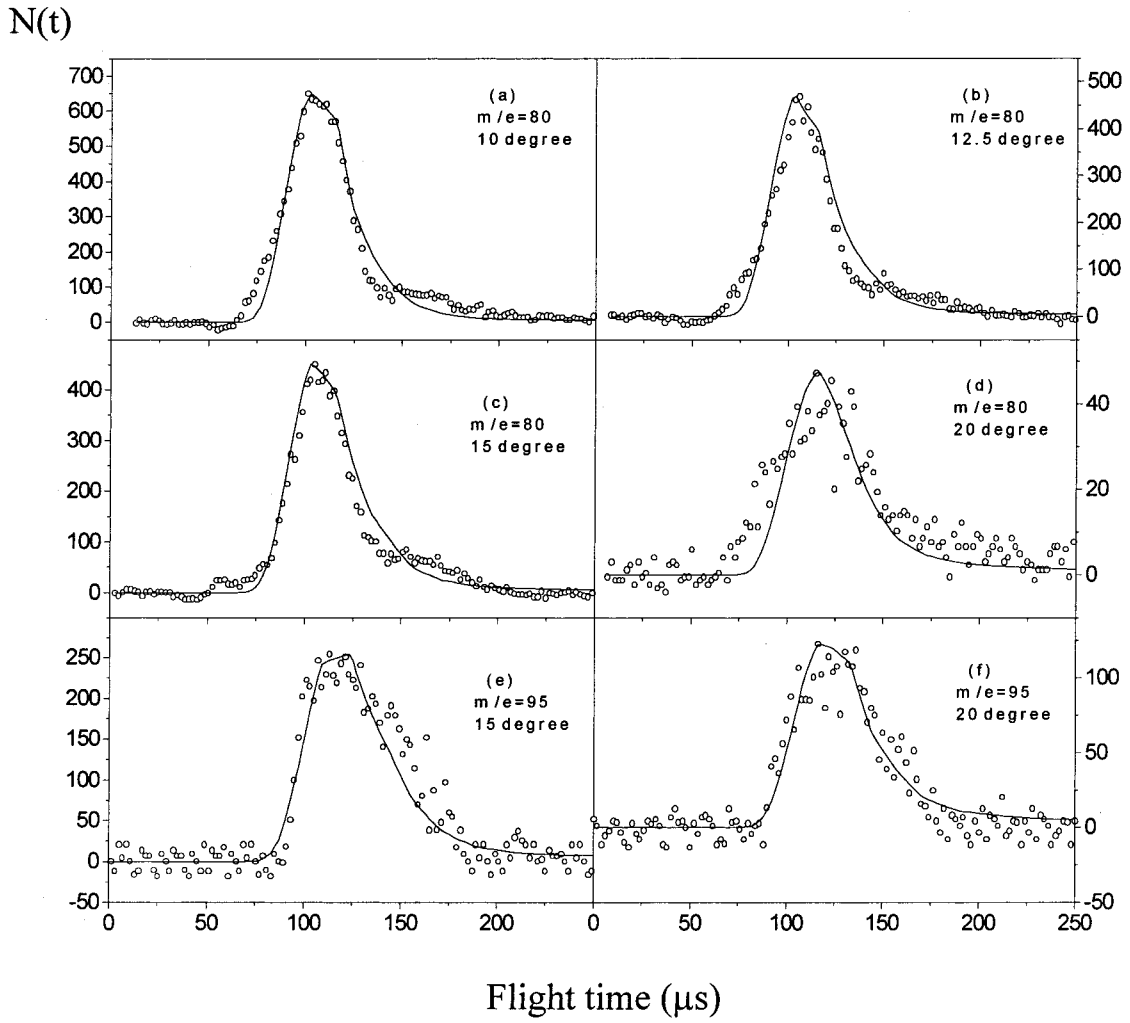

Figure 1. The TOF spectra of 1-bromo-3-fluorobenzene photodissociation at 266 nm $m/e = 80$ corresponding to Br detected at laboratory angles of 10° (a), 12.5° (b), 15° (c), 25° (d) and $m/e = 95$ corresponding to FC_6H_5 of 15° (e), 20° (f). Open circles are the experimental points. Solid line is the best fit by using the total translational energy distribution $P(E_t)$ shown in Figure 4(A) and $\beta = 0.7 \pm 0.1$.

E_{int} tends to be minimal. If the $(E_{int})_{min}$ would be zero, then

$$D_0(\text{C}-\text{Br}) \approx h\nu - (E_t)_{max} \quad (5)$$

For 1-bromo-3-fluorobenzene, the value of $(E_t)_{max}$ is 121.2 ± 4.0 kJ/mol and D_0(C−Br) approximately equals 328.8 ± 4.0 kJ/mol. About 46.8 ± 3.3% of the available energy is partitioned into the translational energy (56.76 ± 4.0 kJ/mol), and thus 53.2 ± 3.3% goes into fragment internal energy. For 1-bromo-4-fluorobenzene, the $(E_t)_{max}$ is 133.8 ± 4.0 kJ/mol and D_0(C−Br) approximately equals to 316.2 ± 4.0 kJ/mol. About 41.7 ± 3.0% of the available energy is partitioned into the translational energy (55.84 ± 4.0 kJ/mol), and thus 58.3 ± 3.0% goes into fragment internal energy.

The C−Br bond strengths of 1-bromo-3-fluorobenzene and 1-bromo-4-fluorobenzene derived from the experimental results are slightly different from that of bromobenzene (342.8 kJ/mol), which may be due to the fact that one of the hydrogen atoms of benzene ring is replaced by a fluorine atom.

4.Discussion

4.1. Photodissociation Mechanisms at 266 nm. To illustrate the photodissociation mechanism, we have optimized the geometries of the ground state, the singlet excited states and the triplet state using the GAUSSIAN 94 package.[63] In the ground state, geometry optimization is performed at the HF/6-31G* level. The geometries of the electronic singlet excited states are optimized using the Hartree−Fock CI singles (CIS) approach with the basis set 6-31G*, in which the excited state function is expanded in the set of singly excited Slater determinants generated by promoting one electron from an occupied orbital to a virtual orbital. For the calculation of the triplet state geometry, the UHF/6-31G* is used. All the geometries are optimized under the constraint of planar configuration and the optimized results are schematically presented in Figure 5 and Figure 6 in standard coordinate. The standard coordinate is defined that the origin of coordinate is the CM of nuclear charge and the coordinate axes are the principal axes of nuclear charge. Nuclear charge is the atomic number; for example, Br is 35, F is 9, C is 6 and H is 1. Moreover, the excitation energies, transition electronic dipole moments and oscillator strengths are presented in Table 2.

According to the calculated results in Table 2, when 1-bromo-3-fluorobenzene and 1-bromo-4-fluorobenzene absorb the 266 nm photon, they should be excited from the S_0 state to the S_1 state despite the fact that the $S_1 \leftarrow S_0$ excitation energies exceed the photon energy, which may be due to the inaccuracy of the calculated results at the CIS level. The $S_1 \leftarrow S_0$ transition electric dipole moment of 1-bromo-3-fluorobenzene is nearly along with the C−Br bond but that of 1-bromo-4-fluorobenzene is almost perpendicular to C−Br bond, which agrees with the experimental results that 1-bromo-3-fluorobenzene is a parallel

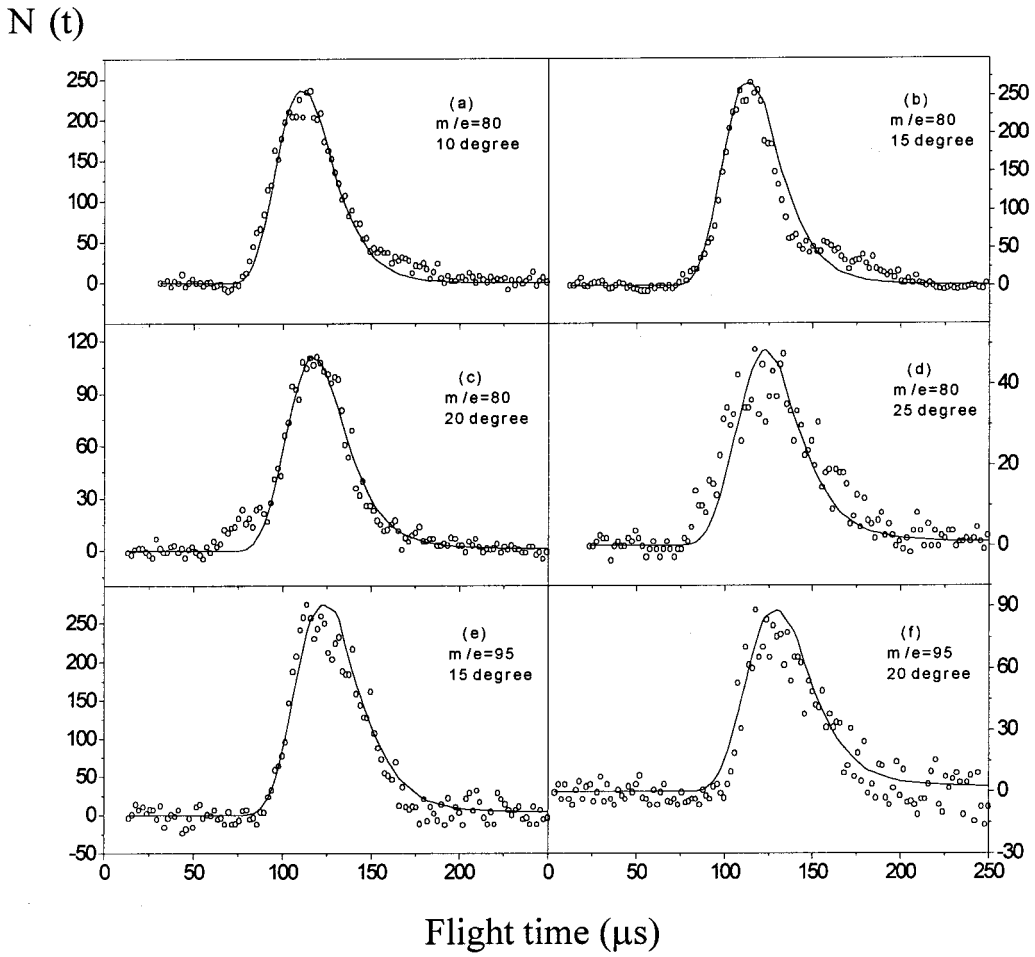

Figure 2. Laboratory TOF spectra of Br ($m/e = 80$) product at detector to beam source angles of 10° (a), 15° (b), 20° (c), 25° (d) and FC_6H_4 ($m/e = 95$) of 15° (e), 20° (f) in the photodissociation of 1-bromo-4-fluorobenzene at 266 nm. Open circles are the experimental points. Solid line is the best fit by using the total translational energy distribution $P(E_t)$ shown in Figure 4(B) and $\beta = -0.4 \pm 0.1$.

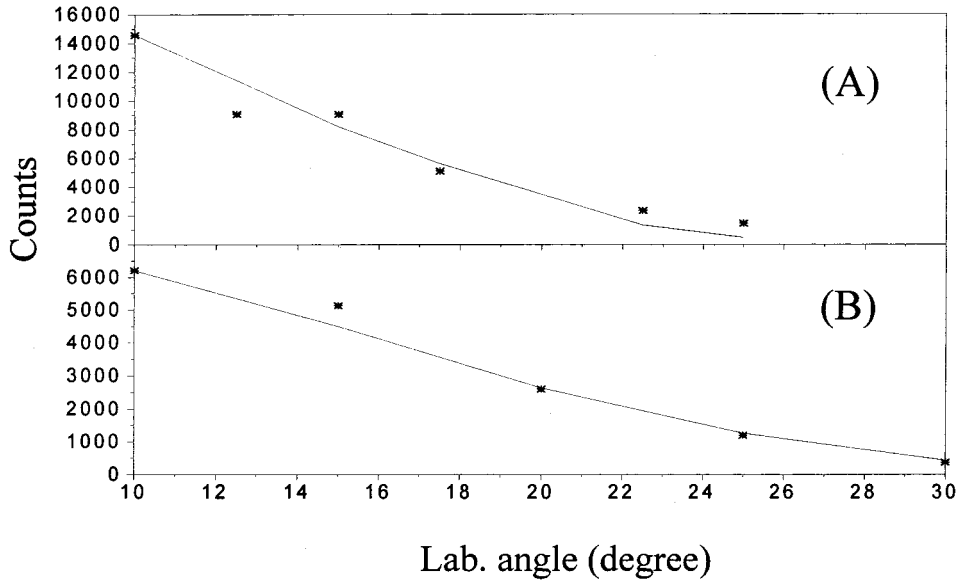

Figure 3. Laboratory angular distribution of the photofragment Br in the photolysis of 1-bromo-3-fluorobenzene (A) and 1-bromo-4-fluorobenzene (B) at 266 nm. Star indicates experimental counts and solid line is the best fitting one by using the total translational energy distribution $P(E_t)$ shown in Figure 4.

transition ($\beta = 0.7 \pm 0.1$) but 1-bromo-4-fluorobenzene is a perpendicular transition ($\beta = -0.4 \pm 0.1$), respectively. By analyzing the CIS density, the $S_1 \leftarrow S_0$ transitions are $\pi^* \leftarrow \pi$ transitions, which are quite obviously seen from Figure 5 and Figure 6. All C−C bond lengths in S_1 states increase by about 0.003 nm; however, the C−Br bonds decrease by about 0.002 nm. Hameka et al.[69] have explained that the excitation involves the promotion of an electron from a bonding π orbital to an antibonding π^* orbital, which leads to a decrease in the rigidity of the benzene ring and reduces the bond order in the majority

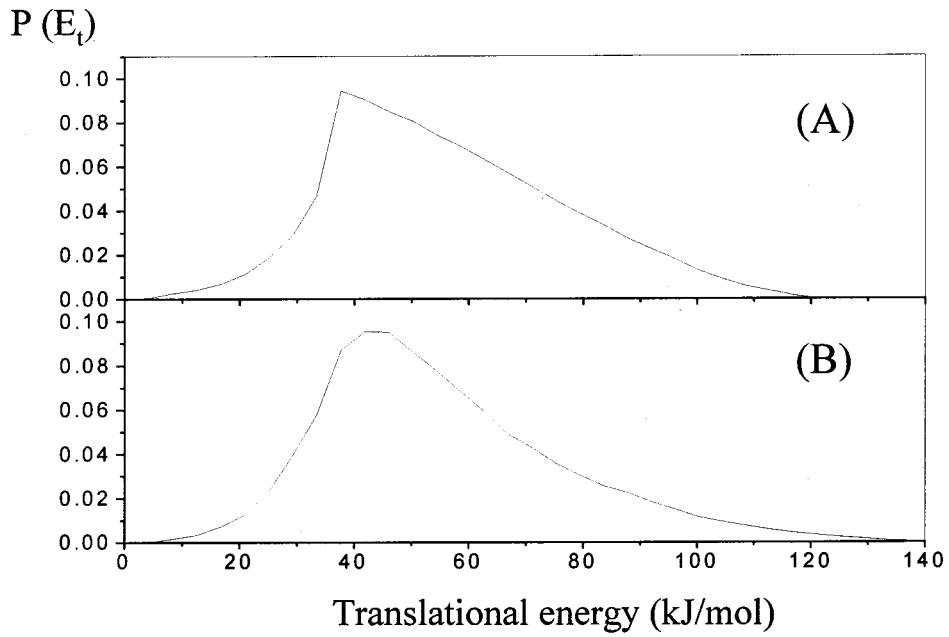

Figure 4. The total center-of-mass translational energy distribution of the photodissociation at 266 nm, (A) and (B) corresponding to 1-bromo-3-fluorobenzene and 1-bromo-4-fluorobenzene, respectively.

of the C−C bonds, thus giving rise to the increase in bond lengths. The optimized results of the triplet excited states (T_1) show that they have stable geometries, and the C−Br bond lengths are almost the same as that of ground electronic states, except that some C−C bond lengths increase, which are also caused by the $\pi^* \leftarrow \pi$ transition.

On the basis of the above experimental results and ab initio calculations, we qualitatively propose the most possible photodissociation mechanism. Since for 1-bromo-3-fluorobenzene and 1-bromo-4-fluorobenzene the C−Br bond lengths in the S_1 state are shorter than that in the S_0 state and the C−Br bond in the T_1 state are approximately equal to that in the S_0 state, the S_1 state and T_1 state should be bound states. Thus the probable dissociation process may be that the parent molecules are excited vertically to the S_1 state by absorbing a photon, then they switch to the high vibrationally excited T_1 state by intersystem crossing and finally dissociate. Clearly this dissociation process is a vibrationally hot molecular dissociation mechanism. This is different from the photodissociation of bromobenzene at 266 nm.[24] For the photolysis of bromobenzene at 266 nm, β is determined to be -0.7 ± 0.2 and the transition dipole moment is almost perpendicular to the C−Br bond. The dissociation mechanism proposed is a fast predissociation process, which is due to the fact that the triplet state T_1 is a repulsive state.

According to the data in Table 3, the fractions into translational energies for the photodissociation of bromide aryl molecules at 266 nm have very similar values. The results are very common for aryl halide photodissociation, for example, for chlorobenzene photodissociation at 193 nm,[30,33] 248 nm[33] and 266 nm,[23] about 24%, 20% and 20% are partitioned into translational energy, respectively.

Recently, Zewail et al.[43,44] proposed that a conical interaction plays an important role in the nonradiative dynamics of large organic molecules in their studies of the photodissociation of iodobenzene. This seems to be a general phenomenon in the photodissociation of aryl halides. Here, the photodissociation processes are slow predissociation, parent molecules both from the initial excited state (S_1) switch to the triplet excited state (T_1) by intersystem crossing. This mechanism was also postulated for the photolysis of benzyl chloride at 193 nm[30] and chlorobenzene at 248 nm[34] as well as chlorobenzene at 266 nm.[23]

4.2. Effect of Substitution. The effect of substitution is very important in aryl halide photolysis, including the mass effect, inductive effect, steric effect and conjugation effect, etc. The most important effect is the inductive effect, which usually determines the molecular character and the photodissociation mechanism. The inductive effect is of two kinds: one is electropositive, or electron-repelling and the other is electronegative, or electron-attracting.

Ichimura, et al.[34] studied the photofragmentation of chlorotoluenes and dichlorobenzenes at 193 nm and discussed the substitution effects of the methyl and chlorine atom. They propose that the substitution effect of the methyl group on the photodecomposition mechanism seems to be attributable to the enhanced intersystem crossing due to the methyl internal rotation, which increases the probability of second channel, i.e. predissociation through the triplet state. This kind of methyl internal rotation effect has been studied for the first time by Okuyama et al.[64] in the S_1 fluorotoluene and recently by Moss and co-workers.[65,66] On the other hand, the mode selectivity of the methyl torsion in intersystem crossing of acetophenone has been studied by Kamei et al.[67] and their results strongly suggest that the internal rotation of the methyl group plays an important role in inducing the intersystem crossing. However, since the methyl is a weak electropositive group, the inductive effect is very weak and the substitution effect is mainly caused by the internal rotation. Moreover, Ichimura et al. imagine that the photodecomposition of dichlorobenzene is in general similar to that of chlorobenzene and declare that additional chlorine substitution in chlorobenzene does not cause the drastic change in the photodecomposition mechanism at 193 nm.[34] Although the chlorine atom is a strong electronegative group, its electric dipole polarizability is a reasonably large and therefore has an n-π electron interaction, which eliminates the electron-attracting effect. Thus the substitution effect of chlorine is not easy to observe experimentally.

The fluorine atom is a very ideal group to study this kind of substitution effect; it has the maximum electron affinity (3.999

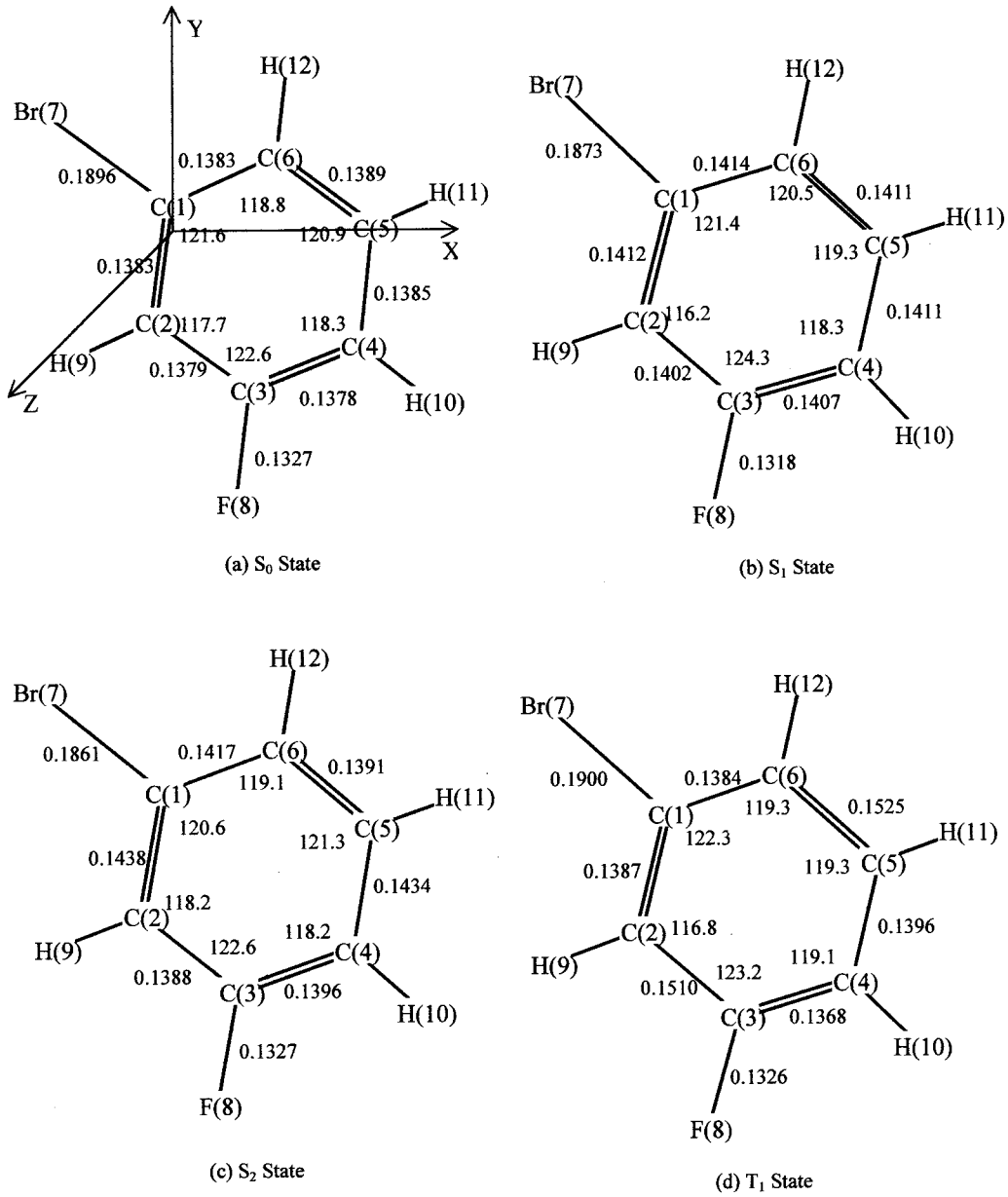

Figure 5. The optimized geometries of 1-bromo-3-fluorobenzene by using Gaussian 94 package: (a) ground state (S_0) at HF/6-31G*, (b) first excited electronic state (S_1) at CIS/6-31G*, (c) second excited electronic state (S_2) at CIS/6-31G*, and (d) the triplet excited state (T_1) at UHF/6-31G*. Bond lengths in nanometer and angles in degrees.

eV) and minor electric dipole polarizability (5.57×10^{-31} m^3),[68,70] whereas those of chlorine atom are 3.615 eV and 2.18×10^{-30} m^3, respectively, and the electron affinity of methyl is 0.08 eV. The dipole moments of bromobenzene, 1-bromo-3-fluorobenzene and 1-bromo-4-fluorobenzene are listed in Table 4. The dipole moment of bromobenzene is the largest and the dipole moment of 1-bromo-3-fluorobenzene is larger than that of 1-bromo-4-fluorobenzene. It is obvious that the electron-attracting ability of fluorine atom is stronger than that of bromine because the electron affinity of fluorine is higher than bromine (3.365 eV) and the dipole polarizability is less than bromine (3.05×10^{-30} m^3), which generates the change of dipole moment, including the direction and value. The transition electron dipole moment can be written as

$$R = \langle \psi_E | \mu \cdot E | \psi_G \rangle \qquad (6)$$

in which R is the transition electron dipole moment, ψ_E and ψ_G are the excited state and ground-state wave functions. μ is the dipole moment and E is electric field vector. The change of the direction of molecule dipole moment may cause the transition electron dipole moment direction different and the anisotropy parameter β value different. This may be one of the reasons why the β values of 1-bromo-3-fluorobenzene and 1-bromo-4-fluorobenzene are different. The other reason may be that the symmetries of ψ_E and ψ_G of 1-bromo-3-fluorobenzene and 1-bromo-4-fluorobenzene are different.

This powerful electron-attracting effect of fluorine atom also attracts electron density from the bromine atom and benzene ring, which causes the C−C bonds in the vicinity of fluorine to be shorter than other C−C bonds and the C−Br bond strengths to decrease. According to the fitted results derived above, the C−Br bond strengths of 1-bromo-3-fluorobenzene and 1-bromo-4-fluorobenzene are lower than that of bromobenzene indeed. The electron-attracting effect of para-substitution by a fluorine atom is stronger than meta-substitution due to the conjugation effect of benzene ring, which causes the C−Br bond length of 1-bromo-4-fluorobenzene to be longer than that of 1-bromo-3-

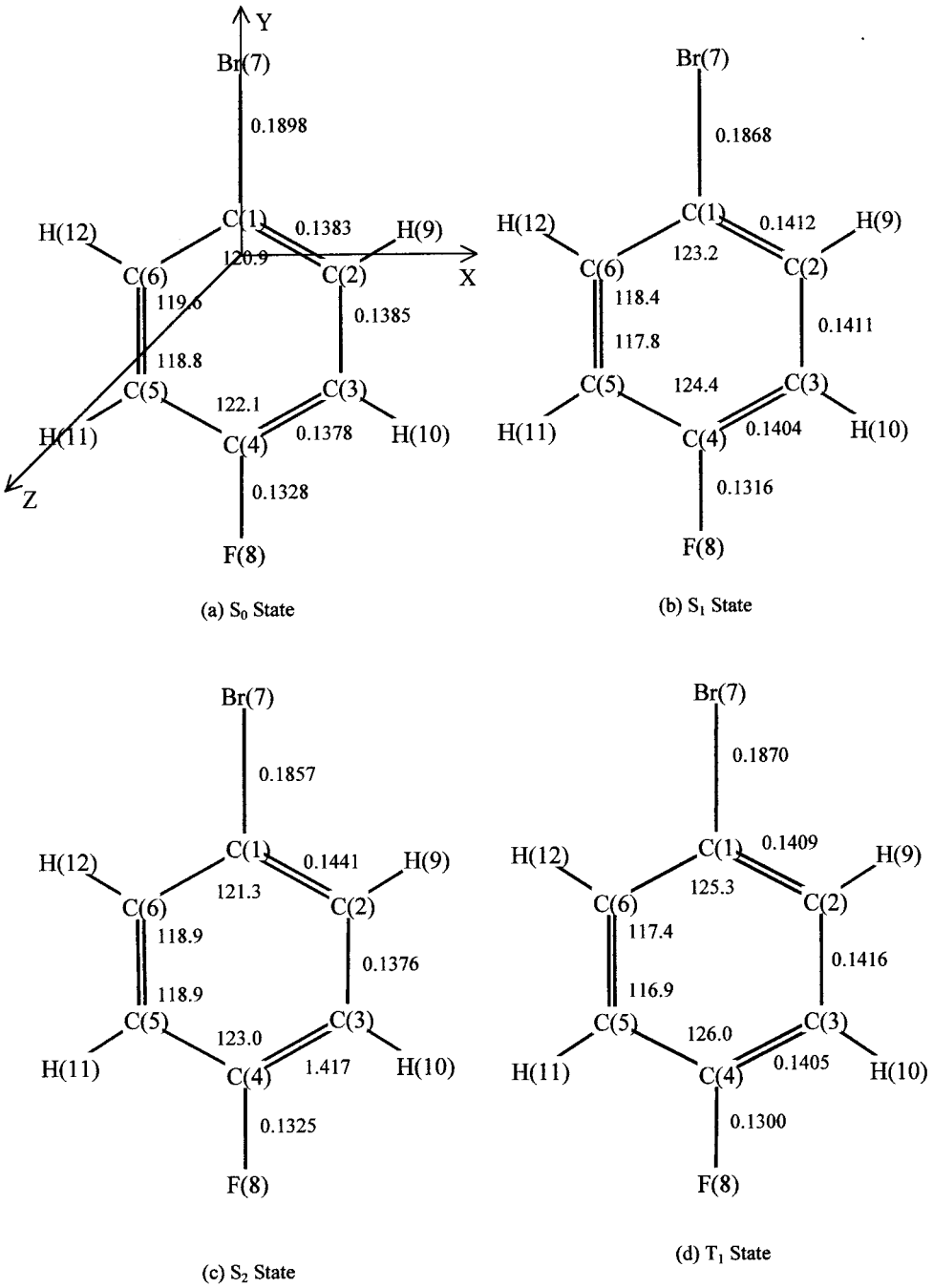

Figure 6. The optimized geometries of 1-bromo-4-fluorobenzene by using GAUSSIAN 94 package. (a) The ground state (S_0) at HF/6-31G*, (b) the first excited electronic state (S_1) at CIS/6-31G*, (c) the second excited electronic state (S_2) at CIS/6-31G*, and (d) the triplet excited state (T_1) at UHF/6-31G*. Bond lengths in nanometers and angles in degree.

TABLE 2: Excitation Energy, Transition Electric Dipole Moment, and Oscillator Strengths Calculated Using GAUSSIAN 94, Corresponding to $S_1 \leftarrow S_0$ and $S_2 \leftarrow S_0$ of 1-Bromo-3-fluorobenzene and 1-Bromo-4-fluorobenzene

			TEDM[b](Au)			
		ΔE^a (nm)	X	Y	Z	OSC.[c]
1-bromo-3-fluorobenzene	$S_1 \leftarrow S_0$	205.77	−0.4816	0.2687	0.0000	0.0449
	$S_2 \leftarrow S_0$	198.27	−0.2912	0.3645	0.0000	0.0333
1-bromo-4-fluorobenzene	$S_1 \leftarrow S_0$	208.19	−0.4677	0.0000	0.0000	0.0319
	$S_2 \leftarrow S_0$	198.41	0.0000	0.3991	0.0000	0.0244

[a] Excitation energy. [b] The transition electric dipole moment in standard coordinate. [c] The oscillator strengths.

fluorobenzene. Referring to the ab initio calculation results, in the ground state (S_0), the C−Br bond length of 1-bromo-4-fluorobenzene (0.1898 nm) is slightly longer than that of 1-bromo-3-fluorobenzene (0.1896 nm). Moreover, the fits to the measured data indicate that the C−Br bond strength of 1-bromo-4-fluorobenzene (≈316.2 ± 4.0 kJ/mol) is slightly lower than that of 1-bromo-3-fluorobenzene (≈328.8 ± 4.0 kJ/mol).

The experimental results presented in Table 3 show that the fragments of bromobenzene have the largest partitioning of translational energy from the available energy (47%). The

TABLE 3: Anisotropy Parameters β and Fractions of Average Translational Energy in Available Energy ($\langle E_t \rangle / E_{Avl}$) of Several Bromated Aryls

	266 nm		193 nm
	β	$\langle E_t \rangle / E_{avl}$	$\langle E_t \rangle / E_{avl}$
bromobenzene[a]	-0.7 ± 0.2	47%	46%[d]
o-bromotoluene[b]	-0.42 ± 0.1	44%	
	0.5 ± 0.2	9%	
p-bromotoluene[c]	-0.4 ± 0.2	38.5%	
1-bromo-3-fluorobenzene	0.7 ± 0.1	$46.8 \pm 3.3\%$	
1-bromo-4-fluorobenzene	-0.4 ± 0.1	$41.7 \pm 3.0\%$	
bromopentafluorobenzene[d]			22%[d]

[a] Data taken from ref 24. [b] Data taken from ref 26. [c] Data taken from ref 27. [d] Data taken from ref 30.

TABLE 4: Dipole Moments of Bromobenzene, 1-Bromo-3-fluorobenzene and 1-Bromo-4-fluorobenzene in Standard Coordinate at Ground State Calculated by GAUSSIAN 94 at HF/6-31G* Level

	dipole moment (Debye)			
	X	Y	Z	total
bromobenzene	0.0000	2.1204	0.0000	2.1204
1-bromo-3-fluorobenzene	1.7723	0.4779	0.0000	1.8356
1-bromo-4-fluorobenzene	0.0001	−0.3920	0.0000	0.3920

decrease of the average translational energy of o,*p*-bromotoluene may be caused by the increase of the photofragment internal energy (the internal degree of freedom increase), including vibrations and rotations, which is due to the substitution of the methyl group. For 1-bromo-3-fluorobenzene and 1-bromo-4-fluorobenzene, in comparison with bromobenzene, the substitution of fluorine does not change the photofragment internal energy (the internal degree of freedom invariable) and thus the fractions of available energy going into translational energy are closer to that of bromobenzene. However, the fluorine atom can change both the CM position of parent molecules and the CM position of the photofragment. The para-position substitution is C_{2v} symmetry, while the meta-position substitution is C_s symmetry. The CM positions of 1-bromo-4-florobenzene and 1-bromo-3-florobenzene greatly deviate from their geometrical centers. For the former, the CM is still located at the line of F−Br, therefore, the repulsive force of the C−Br bond breakage will excite the p−C_6H_4F fragment to higher vibrationally excited states. However, for the latter, the CM is not located in the line of F−Br and C−Br, and the *m*-C_6H_4F fragment will be excited to higher rotationally excited states mainly. This may be one of the reasons why the average translational energy of 1-bromo-4-florobenzene (55.84 ± 4.0 kJ/mol) is lower than that of 1-bromo-3-florobenzene (56.76 ± 4.0 kJ/mol) for photodissociation at 266 nm.

In Table 3, it can be seen distinctly that the fraction of available energy going into translational energy for 1-bromo-4-fluorobenzene is approximately 5% less than that of 1-bromo-3-fluorobenzene. The other reasons that result in the differences of the fragment translational energy of both 1-bromo-4-fluorobenzene and 1-bromo-3-fluorobenzene probably include the different S_0, T_1, and S_1 potential energy surfaces and geometries and so on. Another typical example of the fluorine substitution effect on photodissociation is the photodissociation of bromopentafluorobenzene and bromobenzene at 193 nm: there is 46% of the available energy going into the fragment translation for photolysis of bromobenzene, whereas there is only 22% of the available energy partitioned into the fragment translation for bromopentafluorobenzene. The strong electron-withdrawing effect will attract electron density from the benzene ring to the fluorine atoms and decrease the electron density in the benzene ring, which results in the C−C bond lengths increasing and the C−C bond strengths decreasing. The steric effect of the fluorine atom also plays an important role due to the covalent radius of the fluorine atom which is 0.072 nm, while that of hydrogen atom is only 0.032 nm, which will make the benzene ring distort and the C−C bonds longer and weaker. Owing to the looseness of benzene ring, more available energy is kept in the internal energy of C_6F_5. This may indicate why the fraction of translational energy of bromopentafluorobenzene photodissociation products is much lower than that of bromobenzene photodissociation at 193 nm. Such phenomena have been observed in the photodissociation of iodobenzene and iodopentafluorobenzene at 193 nm[30] as well.

The different position substituent effects of the aryl halides are also seen from the photodissociation of bromotoluene at 266 nm. The photodissociation of *p*-bromotoluene at 266 nm only has one dissociation channel, whereas *o*-bromotoluene has two photodissociation channels. Due to the fact that the volume of methyl is relatively large, the steric effect may play an important role. When the methyl is ortho substitution, the interaction of methyl and bromine is very strong, which leads to the distortion of benzene ring, restrains the rotation of methyl, decelerates the velocity of intersystem crossing and results in more parent molecules turning into the ground state by internal conversion. Therefore, a second dissociation channel emerges for *o*-bromotoluene. However, when methyl is para substituted, the steric interaction between methyl and bromine is the weakest, therefore, the intersystem conversion will be very fast and the second channel disappears.

5. Conclusions

Using photofragment translational spectroscopy on a universal crossed molecular beam machine, we have studied the photodissociation of 1-bromo-3-fluorobenzene and 1-bromo-4-fluorobenzene at 266 nm under collision-free conditions. Angle-resolved Br and FC_6H_5 photofragment TOF spectra are measured. For 1-bromo-3-fluorobenzene, about $46.8 \pm 3.3\%$ of the available energy partitions into photofragment translation energy and the anisotropy parameter β is determined to be 0.7 ± 0.1, which indicates that a parallel transition is dominant. For 1-bromo-4-fluorobenzene, it is about $41.7 \pm 3.0\%$ and β is -0.4 ± 0.1 which indicates that perpendicular transition acts as an essential role. The possible photodissociation mechanism, has been proposed, i.e., dissociation by intersystem crossing from S_1 to T_1. The fluorine atom substitution effect is discussed as well.

Acknowledgment. This work is supported by Outstanding Young Scientist Awards of National Natural Science Foundation of China (NO. 29825107), and NKBRSF. We thank Professor Yuan T. Lee, R. N. Dixon, Cheuk-Yiu Ng, Xinshen Zhao and Xueming Yang for supplying the CMLAB2 program and giving helpful advice.

References and Notes

(1) Simons, J. P. *J. Phys. Chem.* **1984**, *88*, 1287.
(2) Leone, S. R. *Adv. Chem. Phys.* **1982**, *50*, 255.
(3) Shapiro, M.; Bersohn, R. *Annu. Rev. Phys. Chem.* **1982**, *33*, 409.
(4) Bush, G. E.; Mahoney, R. T.; Morse, R. I.; Wilson, K. R. *J. Chem. Phys.* **1969**, *51*, 449.
(5) Bush, G. E.; Cornelius, J. F.; Mahoney, R. T.; Morse, R. I.; Schlosser, D. W.; Wilson, K. R. *Rev. Sci. Instrum.* **1970**, *14*, 1066.
(6) Bush, G. E.; Wilson, K. R. *J. Chem. Phys.* **1972**, *56*, 3626, 3638, 3655.
(7) Ashfold, M. N. R.; Lambert, I. R.; Mordaunt, D. H.; Morley, G. P.; Western, C. M. *J. Phys. Chem.* **1992**, *96*, 2938.

(8) Minton, T. K.; Nelson, C. M.; Moore, T. A.; Okumura, M. *Science* **1992**, *258*, 1342.
(9) Butler, L. J.; Neumark, D. M. *J. Phys. Chem*. **1996**, *100*, 12801.
(10) Bersohn, R. *IEEE J. Quantum Electron*. **1980**, *16*, 1208.
(11) Bersohn, R. *J. Phys. Chem*. **1984**, *88*, 5145.
(12) Wodtke, A. M.; Lee, Y. T. in Ashfold, M. N. R.; Baggott, J. E. (Eds.), *Molecular Photodissociation Dynamics*, Royal Society of Chemistry, London, 1987; P. 31.
(13) Jonah, C. *J. Chem. Phys*. **1971**, *55*, 1915.
(14) Zare, R. N. *Mol. Photochem.* **1971**, *55*, 1.
(15) Yang, S.; Bersohn, R. *J. Chem. Phys*. **1974**, *61*, 4400.
(16) Dzvonik, M.; Yang, S.; Bersohn, R. *J. Chem. Phys*. **1974**, *61*, 4408.
(17) Spark, R. K.; Carlson, L. R.; Shobatake, K.; Kowalczyk, M. L.; Lee, Y. T. *J. Chem. Phys.* **1980**, *72*, 1401.
(18) Wodtke, A. M.; Lee, Y. T. *J. Phys. Chem*. **1985**, *89*, 4744.
(19) Continetti, R. E.; Balko, B. A.; Lee, Y. T. *J. Chem. Phys*. **1988**, *89*, 3383.
(20) Van veen, G. N. A.; Mohamed, K. A.; Baller, T.; de Vries, A. E. *Chem. Phys.* **1983**, *74*, 261.
(21) Xu, Z.; Koplitz, B.; Wittig, C. *J. Chem. Phys.* **1989**, *90*, 2692.
(22) Krautwald, H. J.; Schnieder, L.; Welge, K. H.; Ashfold, M. N. R. *Faraday Discuss. Chem. Phys. Soc*. **1986**, *82*, 99.
(23) Wang, G. J.; Zhu, R. S.; Zhang, H.; Han, K. L.; He, G. Z.; Lou, N. Q. *Chem. Phys. Lett.* **1998**, *288*, 429.
(24) Zhang, H.; Zhu, R. S.; Wang, G. J.; Han, K. L.; He, G. Z.; Lou, N. Q. *J. Chem. Phys.* **1999**, *110*, 2922.
(25) Wang, G. J.; Zhang, H.; Zhu, R. S.; Han, K. L.; He, G. Z.; Lou, N. Q. *Chem. Phys*. **1999**, *241*, 213.
(26) Zhu, R. S.; Zhang, H.; Wang, G. J.; Han, K. L.; He, G. Z.; Lou, N. Q. *Chem. Phys. Lett.* **1999**, *313*, 98.
(27) Zhang, H.; Zhu, R. S.; Wang, G. J.; Han, K. L.; He, G. Z.; Lou, N. Q. *Chem. Phys. Lett*. **1999**, *300*, 483.
(28) Zhu, R. S.; Zhang, H.; Wang, G. J.; Han, K. L.; He, G. Z.; Lou, N. Q. *Chem. Phys.* **1999**, *248*, 285.
(29) Kawasaki, M.; Lee, S. J.; Bersohn, R. *J. Chem. Phys.* **1977**, *66*, 2647.
(30) Freedman, A.; Yang, S. C.; Wawasaki, M.; Bersohn, R. *J. Chem. Phys.* **1980**, *72*, 1028.
(31) Ichimura, T.; Mori, Y.; Shinohara, H.; Nishi, N. *Chem. Phys. Lett.* **1985**, *122*, 51.
(32) Ichimura, T.; Mori, Y.; Shinohara, H.; Nishi, N. *Chem. Phys. Lett.* **1985**, *122*, 55.
(33) Ichimura, T.; Mori, Y.; Shinohara, H.; Nishi, N. *Chem. Phys.* **1994**, *189*, 117.
(34) Ichimura, T.; Mori, Y.; Shinohara, H.; Nishi, N. *J. Chem. Phys.* **1997**, *107*, 835.
(35) Hwang, H. J.; EI−Sayed, M. A. *J. Chem. Phys.* **1992**, *96*, 856.
(36) Okabe, H. *In Photochemistry of Small Molecules* (Wiley-Interscience. New York. 1978).
(37) Kawasaki, M.; Kasatani, K.; Sato, H.; Shinohara, H.; Nishi, N. *Chem. Phys.* **1984**, *88*, 135.
(38) Van Veen, G. N. A.; Baller, T.; de Vries, A. E. *Chem. Phys.* **1985**, *92*, 59.
(39) Sparks, R. K.; Shobatake, K.; Carlson, L. R.; Lee, Y. T. *J. Chem. Phys.* **1981**, *75*, 3838.
(40) Barry, M. D.; Gorry, P. A. *Mol. Phys.* **1984**, *52*, 461.
(41) Butler, L. J.; Hintsa, E. J.; Lee, Y. T. *J. Chem. Phys.* **1986**, *84*, 4104.
(42) Butler, L. J.; Hintsa, E. J.; Shane, S. F.; Lee, Y. T. *J. Chem. Phys.* **1987**, *86*, 2051.
(43) Cheng, P. Y.; Zhong, D.; Zewail, A. H. *Chem. Phys. Lett.* **1995**, *237*, 399.
(44) Zhong, D.; Zewail, A. H. *J. Phys. Chem. A* **1998**, *102*, 4031.
(45) Van veen, G. N. A.; Baller, T.; de Vries, A. E.; Van veen, N. J. A. *Chem. Phys.* **1984**, *87*, 405.
(46) Van veen, G. N. A.; Baller, T.; de Vries, A. E. *Chem. Phys.* **1985**, *97*, 179.
(47) Black, J. F.; Powis, I. *Chem. Phys.* **1988**, *125*, 375.
(48) Paterson, C.; Godwin, F. G.; Gorry, P. A. *Mol. Phys.* **1987**, *60*, 729.
(49) Godwin, F. G.; Paterson, C.; Gorry, P. A. *Mol. Phys*. **1987**, *61*, 827.
(50) Ogorzalek Loo, R.; Hall, G. E.; Haerri, H. P.; Houston, P. L. *J. Chem. Phys.* **1989**, *90*, 4222.
(51) Zhu, Q.; Cao, J. R.; Wen, Y.; Zhang, J.; Zhong, X.; Huang, Y.; Fang, W.; Wu, X. *Chem. Phys. Lett.* **1988**, *144*, 486.
(52) Nathanson, G. M.; Minton, T. K.; Shane, S. F.; Lee, Y. T. *J. Chem. Phys.* **1989**, *90*, 6157.
(53) Minton, T. K.; Nathanson, G. M.; Lee, Y. T. *J. Chem. Phys*. **1987**, *86*, 1991.
(54) Kawasaki, M.; Lee, S. J.; Bersohn, R. *J. Chem. Phys.* **1977**, *66*, 2647.
(55) Qi, J. X. Ph.D. Thesis, Dalian Institute of Chemical Physics, Chinese Academy of Sciences, Dalian 1993.
(56) Vernon, M. KELVIN Rare Gas Time-of-Flight Program, Lawrence Berkeley Laboratory Report No. 12422 1981.
(57) Krajnovich, D. J., Ph.D. Thesis, University of California, Berkeley 1983.
(58) Hintsa, E. J.; Zhao, X.; Lee, Y. T. *J. Chem. Phys.* **1990**, *92*, 2280.
(59) Zhao, X., Ph.D. Thesis, University of California, Berkeley 1988.
(60) Zare, R. N. *Mol. Photochem.* **1972**, *4*, 1.
(61) Zare, R. N. Ph.D. Thesis, Harvard University, 1964.
(62) Bersohn, R.; Lin, S. H. *Adv. Chem. Phys.* **1969**, *16*, 67.
(63) Gaussian 94, Revision B.2, Frisch, M. J.; Trucks, G. W.; Schlegel, H. B.; Gill, P. M. W.; Johnson, B. G.; Robb, M. A.; Cheeseman, J. R.; Keith, T. et al. Gaussian, Inc., Pittsburgh, PA, 1995.
(64) Okuyama, K.; Mikami, N.; Ito, M. *J. Phys. Chem.* **1995**, *89*, 5617.
(65) Moss, D. B.; Partenter, C. S.; Ewing, G. E. *J. Chem. Phys.* **1987**, *86*, 51.
(66) Moss, D. B.; Partenter, C. S. *J. Chem. Phys.* **1993**, *98*, 6897.
(67) Kamei, S.; Kuyama, K.; Abe, H.; Mikami, N.; Ito, M. *J. Phys. Chem.* **1986**, *90*, 93.
(68) Weast, R. C. *Handbook of Chemistry and physics* (Chemical Rubber, Cleveland, 1972); Benson, S. W. *Thermochemical Kinetics* (Wiley: New York, 1968).
(69) Hameka, H. F.; Jenson, J. O. *J. Mol. Struct.: THEOCHEM* **1995**, *203*, 331
(70) Hotop, H.; Lineberger, W. C. *J. Phys. Chem.* Ref. Data, **1985**, *14*, 731; Miller, T. M.; Bederson, B. *Adv. At. Mol. Phys.* **1977**, *13*, 1; Drzaic, P. S.; Marks, J.; Brauman, J. L. *in Gas-Phase Ion Chemistry*, Vol. 3, Bowers, M. T. Ed., Academic Press: Orlando, **1984**, p 167.